

Electronic supplementary information

Highly Efficient Bipolar Host Materials towards Solution-Processable Blue and Green Thermally Activated Delayed Fluorescence Organic Light Emitting Diodes

Mallesham Godumala,^{‡a} Suna Choi,^{‡a} Seong Keun Kim,^b Si Woo Kim,^b Jang Hyuk Kwon,^b Min Ju Cho^a and Dong Hoon Choi^{*a}

^a Department of Chemistry, Research Institute for Natural Sciences, Korea University, 145 Anam-ro, Seongbuk-gu, Seoul, 02841, Republic of Korea.

^b Department of Information Display, Kyung Hee University, 26, Kyungheedae-ro, Dongdaemun-gu, Seoul, 02447, Republic of Korea

*Email: dhchoi8803@korea.ac.kr

Fax: +82-2-925-4284, Tel: +82-2-3290-3140

[‡] Both the authors have equally contributed to this work.

Figures and Tables

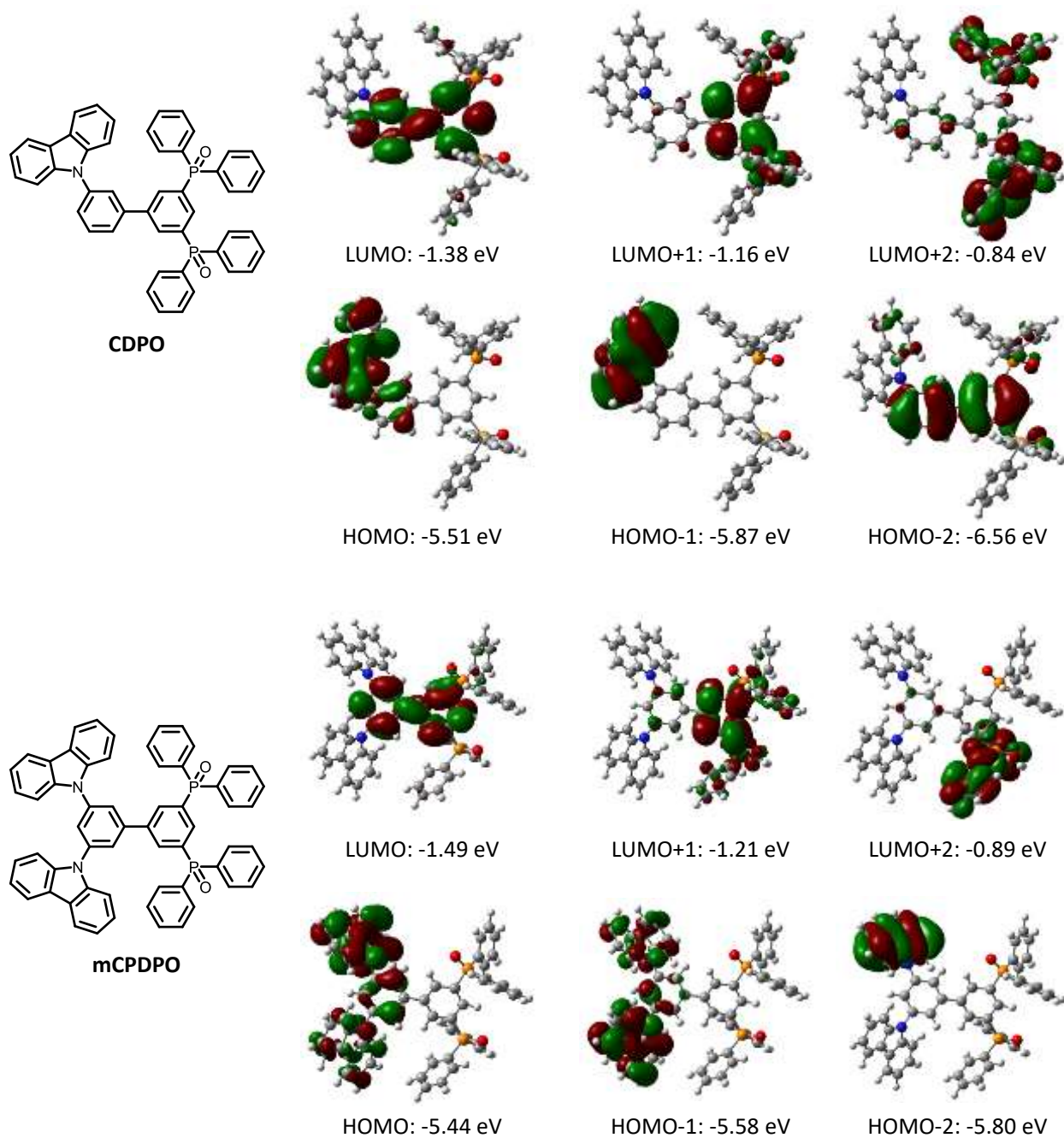


Fig. S1 Spatial distributions of the molecular orbitals in **CDPO** and **mCPDPO**.

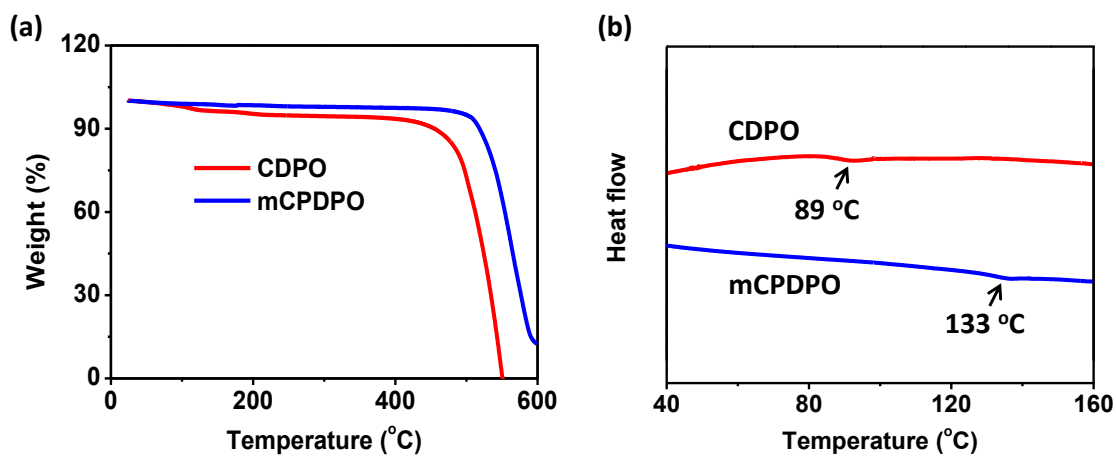


Fig. S2 TGA (a) and DSC (b) plots of CDPO and mCPDPO.

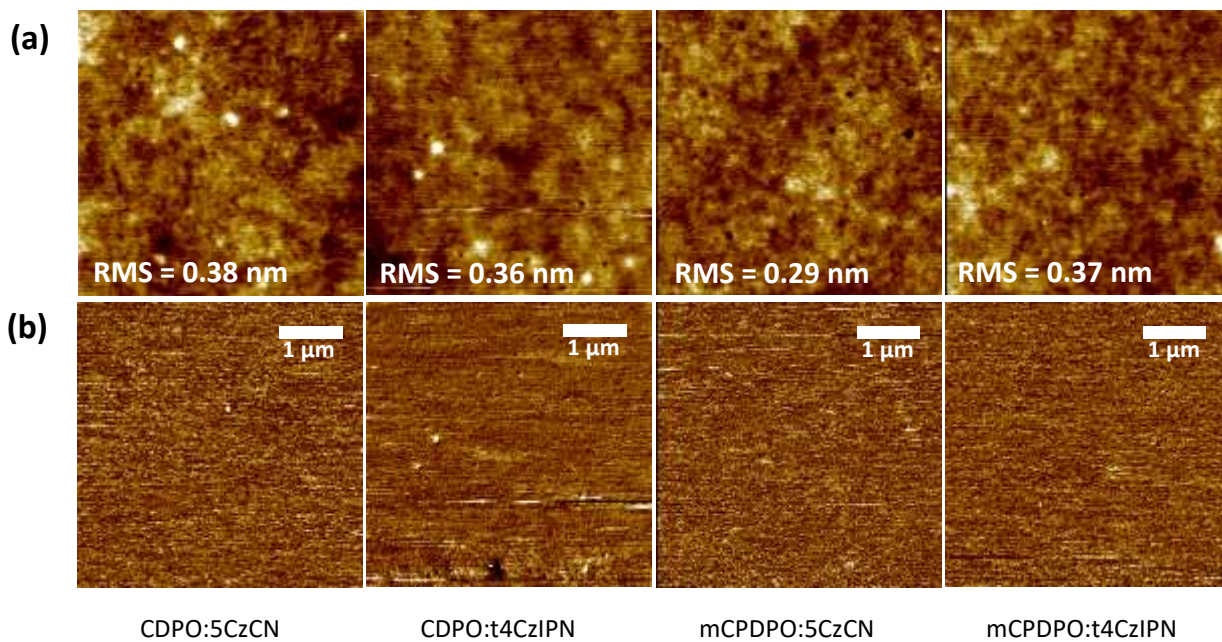


Fig. S3 AFM (a) topography and (b) phase images (5 x 5 μm) of the blend films.

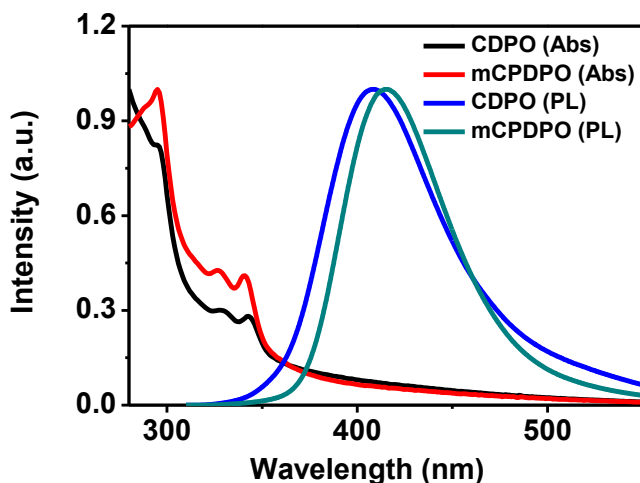


Fig. S4 UV-Vis absorption and PL spectra for **CDPO** and **mCPDPO** in film state.

Table S1. Photophysical properties of the blend films.

Host	Dopant	τ_p (ns) ^a	τ_d (μ s) ^b	k_p (10^7 s ⁻¹) ^c	k_d (10^7 s ⁻¹) ^d	Φ_{PL} (%) ^e
CDPO	5CzCN	16.0	10.7	6.1	9.3	68.1
mCPDPO	5CzCN	16.0	13.7	6.1	7.3	73.4
CDPO	t4CzIPN	16.0	7.1	6.1	14.1	41.8
mCPDPO	t4CzIPN	14.0	8.0	7.1	12.5	60.1

^a Prompt lifetime. ^b Delayed lifetime. ^c Prompt fluorescence decay constant. ^d Delayed fluorescence decay rate constant. ^e Total absolute PL quantum yield measured using integrating sphere.

To investigate the electrochemical properties, cyclic voltammetry measurements were performed for the two new hosts (**CDPO** and **mCPDPO**) in their thin films using a three-electrode electrochemical cell (Fig. S5a). During the anodic sweep, the two compounds undergo quasi-reversible oxidation originating from the carbazole entity. The oxidation onset potentials (E_{ox}^{onset}) of **CDPO** and **mCPDPO** were 1.24 and 1.25 V (vs. Fc/Fc⁺), respectively. The HOMO energies were determined from their E_{ox}^{onset} and the LUMO energy levels were determined by adding the HOMO energy values to their optical bandgaps (E_g).

Cyclic voltammetry measurements were also performed to the two TADF emitters of 5CzCN and t4CzIPN in film states (Fig. S5b). The oxidation onset potential (E_{ox}^{onset}) of 5CzCN and t4CzIPN were observed to be 1.44 and 1.30 V (vs. Fc/Fc⁺), respectively. The HOMO levels of 5CzCN and t4CzIPN were

calculated to be -5.88 and -5.74 eV, respectively. The optical bandgaps obtained from absorption thresholds in film state to be 2.71 and 2.49 eV for 5CzCN and t4CzIPN, respectively. The LUMO energy levels were ascertained by adding the HOMO energy values to their optical bandgaps (E_g) to be -3.17 eV for 5CzCN and -3.25 eV for t4CzIPN.

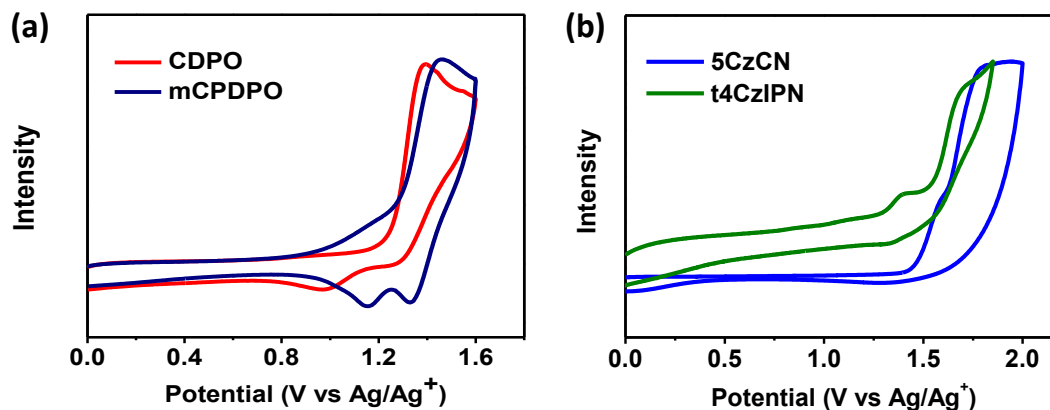


Fig. S5 Cyclic voltammograms of the (a) two hosts, and (b) two TADF emitters in film states.

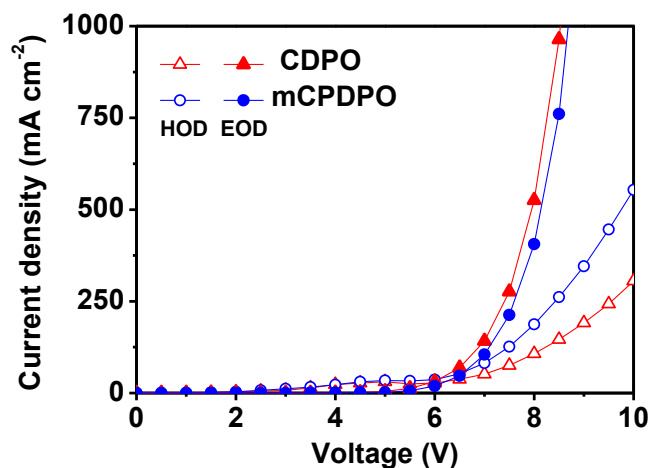


Fig. S6 Hole-only and electron-only devices of CDPO and mCPDPO.

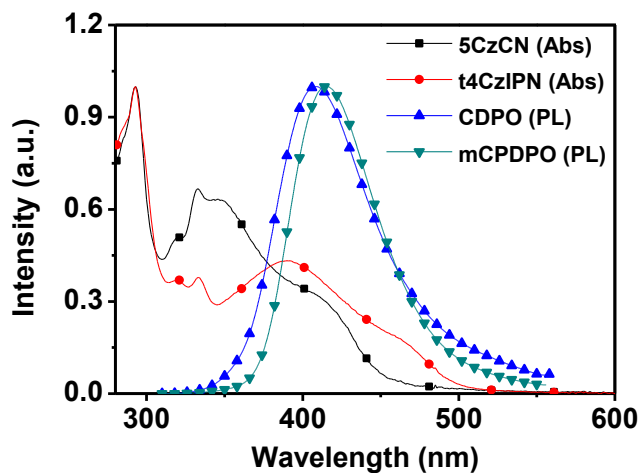


Fig. S7 UV-Vis absorption spectra of 5CzCN and t4CzIPN emitters and PL spectra of **CDPO** and **mCPDPO** hosts in film state.

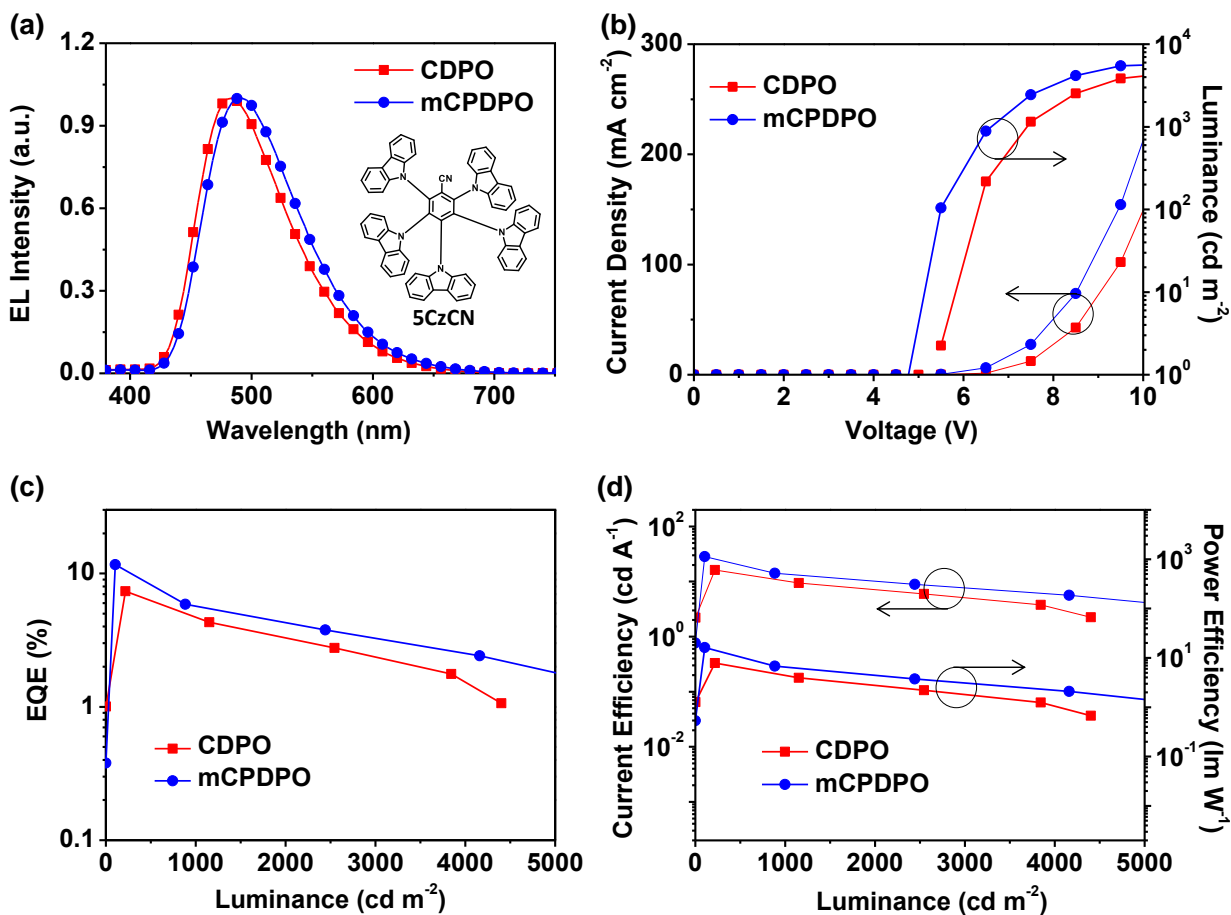


Fig. S8 Characteristics of blue TADF-OLED devices for **CDPO:5CzCN** (25 wt%) and **mCPDPO:5CzCN** (40 wt%); (a) EL spectra (measured at 1000 cd m⁻²), (b) current density–voltage–luminance (*J–V–L*), (c) EQE versus luminance, and (d) current efficiency and power efficiency versus luminance plots.

To verify the EL emission shifts, the PL spectra of two TADF emitters such as 5CzCN and t4CzIPN were measured in their neat and blended films (Fig. S9). As shown in Fig. S9, the PL spectra of two emitters were blue shifted in the host environment compared to their neat films because of the reduced intermolecular interactions. The 5CzCN, **CDPO:5CzCN** (40 wt%) and **mCPDPO:5CzCN** (25 wt%) showed their PL emission at 506, 496 and 494 nm, respectively. Although, **mCPDPO** is rather more polar nature the PL spectrum of **mCPDPO: 5CzCN** (25 wt%) was 2 nm blue shifted because of low dopant concentration. The t4CzIPN, **CDPO:t4CzIPN** (2 wt%) and **mCPDPO:t4CzIPN** (2 wt%) showed their PL emission at 540, 531 and 535 nm, respectively. The 4 nm red shifted emission of **mCPDPO:t4CzIPN** (2 wt%) evidenced by the more polar nature of mCPDPO.

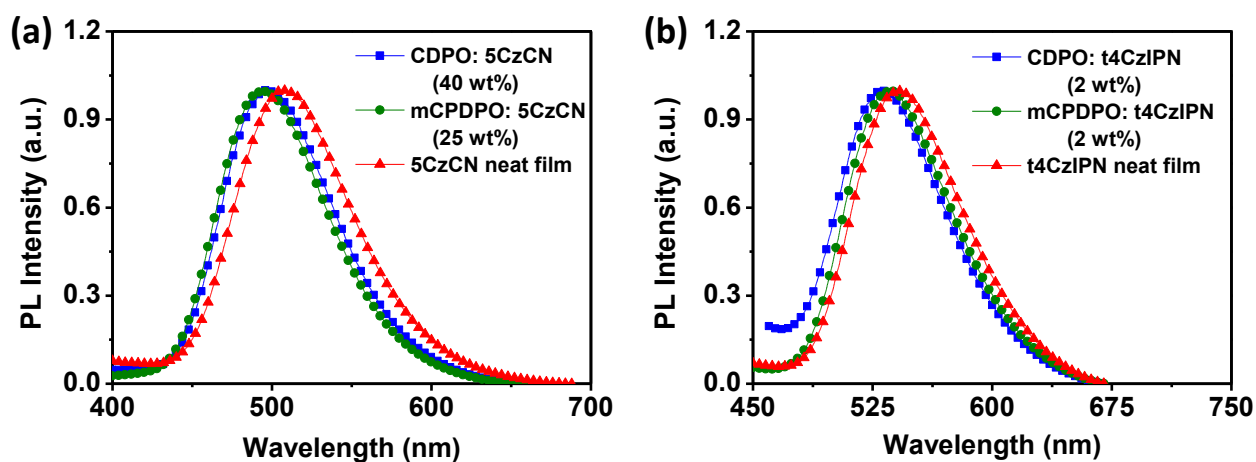


Fig. S9 PL spectra of non-doped doped films of (a) 5CzCN, and (b) t4CzIPN.

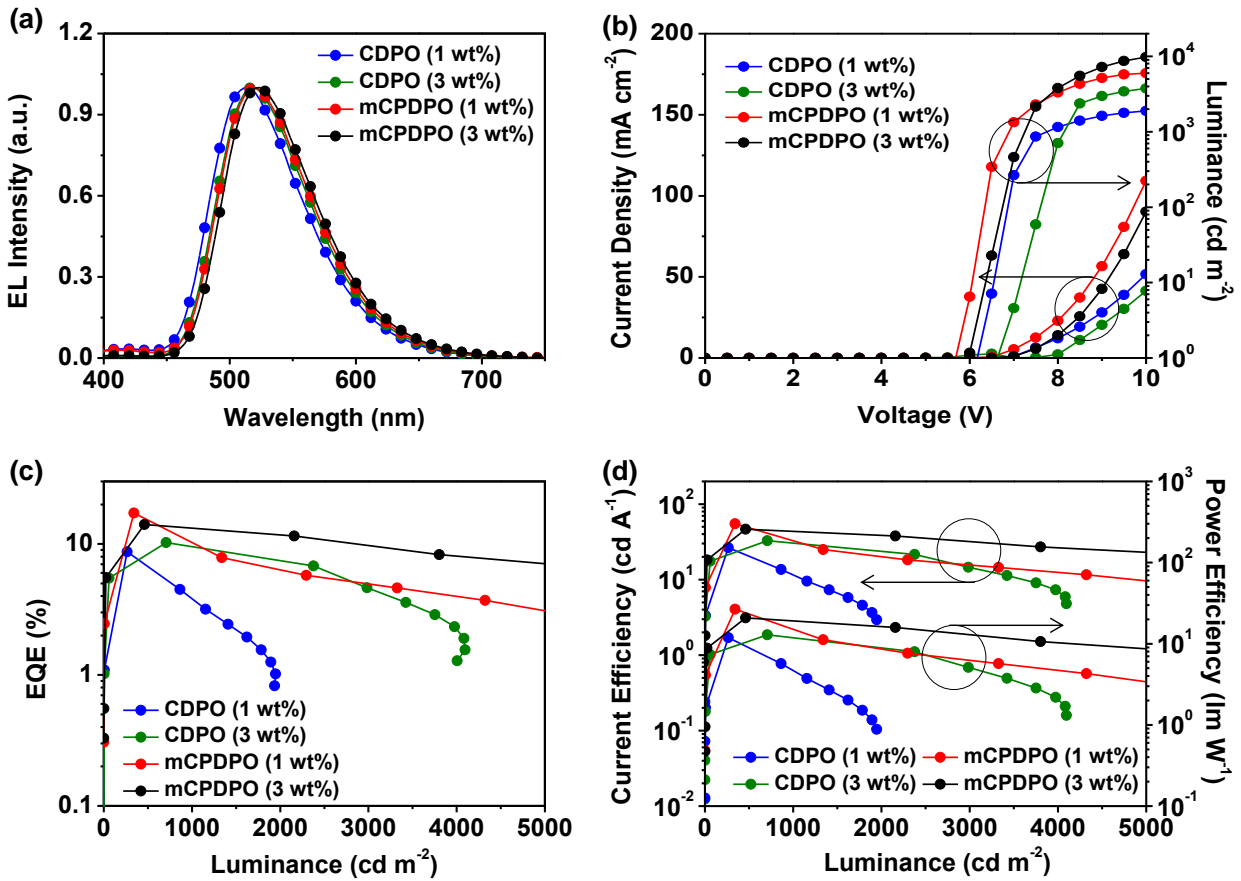


Fig. S10 Characteristics of green TADF-OLED devices for **CDPO** and **mCPDPO** at different doping concentrations: (a) EL spectra (measured at 1000 cd m⁻²), (b) current density–voltage–luminance (J – V – L), (c) EQE *versus* luminance, and (d) current efficiency and power efficiency *versus* luminance plots.

Table S2. CDPO and mCPDPO as hosts and t4CzIPN as a green emitter based TADF-OLED performance data.

Host	Dopant	Dopant conc. (wt%)	Current Efficiency (cd A ⁻¹)			Power Efficiency (lm W ⁻¹)			Quantum Efficiency (%)			CIE ^a (x,y)
			max	100 cd m ⁻²	500 cd m ⁻²	max	100 cd m ⁻²	500 cd m ⁻²	max	100 cd m ⁻²	500 cd m ⁻²	
CDPO	5CzCN	25	16.2	8.5	14.1	7.8	4.2	6.6	7.4	3.9	6.4	(0.19, 0.34)
mCPDPO	5CzCN	40	28.3	26.7	21.2	16.1	15.7	11.4	11.7	11.3	8.8	(0.21, 0.39)
CDPO	t4CzIPN	1.0	26.5	11.7	21.4	11.9	5.3	9.4	8.7	3.8	7.0	(0.27, 0.54)
CDPO	t4CzIPN	3.0	32.8	18.5	27.9	12.9	7.7	11.1	10.3	5.8	8.7	(0.29, 0.57)
mCPDPO	t4CzIPN	1.0	55.1	21.0	50.4	26.6	10.4	24.4	17.2	6.6	15.7	(0.29, 0.57)
mCPDPO	t4CzIPN	3.0	46.5	23.1	46.3	20.1	11.0	20.6	14.1	7.0	14.0	(0.31, 0.58)

^a At a luminance of 1000 cd m⁻².